Journal of Physics and Its Applications

Journal homepage : https://ejournal2.undip.ac.id/index.php/jpa/index

HVSR Microtremor Resonance Frequency and Amplification Analysis Using Earthquake Data for Seismic Hazard Mitigation in Lombok Island

Edy Santoso[1,2], Mohammad Syamsu Rosid[1*], Sigit Pramono[2], Frilla Renty Tama Saputra[3], Daryono[4], and Setyoajie Prayoedhie[2]

[1]*Department of Physics, Faculty of Mathematics and Natural Sciences, Universitas Indonesia, Depok, Indonesia*
[2]*Directorate of Engineering Seismology, Potential Geophysics, and Time Services, Agency for Meteorology, Climatology, and Geophysics (BMKG), Jakarta, Indonesia*
[3]*Research Center for Geological Disaster, Agency for Research and Innovation (BRIN), Tangerang Selatan, Indonesia*
[4]*Directorate of Earthquake and Tsunami, Agency for Meteorology, Climatology, and Geophysics (BMKG), Jakarta, Indonesia*

Corresponding author: *syamsu.rosid@ui.ac.id*

ARTICLE INFO

Article history:
Received: 30 December 2025
Accepted: 18 March 2026
Available online: 30 May 2026

Keywords:
HVSR
Resonance Frequency (f_0)
Amplification (A_0)
Lombok, Indonesia

ABSTRACT

Lombok Island exhibits high seismicity driven by the complex interaction between the subduction of the Indo-Australian plate beneath the Eurasian plate and the activity of the Flores Back-arc Thrust. In seismic hazard mitigation, the Horizontal-to-Vertical Spectral Ratio (HVSR) technique is a fundamental tool for estimating site effects. However, the validity of parameters derived from ambient noise (MHVSR) versus earthquake records (EHVSR) remains a subject of geophysical debate, particularly in regions with high structural heterogeneity. This research evaluates the reliability of resonance frequency (f_0) and amplification factor (A_0) by conducting a direct comparison between MHVSR and EHVSR datasets. Seismic data from seven BMKG stations across Lombok were meticulously selected and processed. The analysis involved windowing and the application of Fast Fourier Transform (FFT) to transition raw waveforms into the frequency domain, allowing for the extraction of stable HVSR spectral curves. The findings reveal a robust correlation between microtremor and earthquake-derived HVSR, with on f_0 ($r = 0.9954$, $\sigma = \pm 0.301$) and A_0 ($r = 0.9232$, $\sigma = \pm 0.748$). Observed minor discrepancies are likely the result of local lithological conditions, wave attenuation, and source-dependent variations such as magnitude or hypocentral distance. Ultimately, this study confirms that ambient vibration HVSR provides dependable estimates of site resonance parameters, aligning with earthquake records within tolerable error margins. These results strengthen the case for microtremor investigations as a reliable, non-invasive method for local seismic hazard evaluation. Such findings are vital for refining seismic hazard mitigation and enhancing urban resilience planning in seismically active zones like Lombok Island.

1. Introduction

In recent years, several studies have addressed the reliability and limitations of microtremor-based HVSR (Horizontal-to-Vertical Spectral Ratio) parameters through direct comparison with earthquake-derived HVSR, highlighting potential underestimation of ground motion amplification characteristics when using ambient vibration alone. Seismic micro zonation in high-risk Lombok Island heavily relies on the practical HVSR method using microtremor data to determine the ground's dominant frequency (f_0) and amplification factor (A_0) [1]-[3]. However, a critical scientific debate questions the reliability of this approach, as results from subtle microtremors may not accurately predict the ground's response during a powerful earthquake [4].

The core issue is that the amplification factor (A_0) derived from microtremors often underestimates the shaking experienced during actual earthquakes, potentially leading to an inaccurate and unsafe assessment of the true hazard [5]. This uncertainty is especially critical for Lombok, where the island's complex geology with sharp contrasts between soft sedimentary deposits and hard volcanic rock can further magnify the discrepancy between microtremor and earthquake responses. Despite these well documented limitations and ongoing debate regarding the interpretation and reliability of microtremor-based HVSR estimates [2], [6], [7], most micro zonation studies in Lombok have adopted the microtremor HVSR method with limited direct validation using locally recorded earthquake data. This creates a crucial research gap: the reliability of Lombok's current seismic hazard maps is empirically untested.

Therefore, the fundamental question remains: do the f_0 and A_0 parameters used for micro zonation accurately reflect the island's true seismic vulnerability? The HVSR method is one of the most practical and commonly used techniques for estimating the soil response characteristics to earthquake shaking, known as the site effect [1]. The primary advantages of the HVSR method lie in its operational simplicity, cost-effectiveness, and its capacity to yield two fundamental seismic

parameters: the resonance frequency (f_0) and the amplification factor (A_0).

The f_0 parameter identifies the dominant frequency at which ground motion is maximally excited, while A_0 quantifies the magnitude of seismic amplification at that specific frequency [8],[9]. Within the complex tectonic setting of Lombok characterized by high seismic activity these parameters are crucial for characterizing site-specific responses. Due to its practicality, the HVSR method, particularly when utilizing microtremor data, has been extensively implemented for seismic micro zonation mapping across Indonesia to enhance regional earthquake resilience [4], [5]. Furthermore, the reliability of these estimates is often validated by comparing A_0 with empirical transfer functions, which typically demonstrate spectral consistency from f_0 up to 25 Hz when local geological constraints are considered [10].

The main issue driving this study is the ongoing scientific debate regarding the reliability and consistency of HVSR results from microtremor data compared to real earthquake data. Although microtremors offer efficiency, the results do not always represent the ground response during a real earthquake. Several studies have shown good agreement between microtremor and earthquake HVSR for both parameters f_0 and A_0 [7]. However, many other studies report significant differences, especially in the amplification factor values (A_0). Specifically, several findings indicate that the value of A_0 microtremor data tends to be underestimated compared to those derived from earthquake recordings [2], [3]. This difference indicates that using microtremor data alone can provide an inaccurate picture of the level of shock amplification hazard, especially during strong earthquakes [8].

The discrepancy between microtremor and earthquake data becomes even more critical in areas with complex and heterogeneous geology. This is where the specific issues raised for the Lombok Island region lie activity, active faults, and sharp variations in soil conditions between soft sedimentary deposits and hard volcanic rocks. Such complex geological conditions can cause significant differences between the subtle vibration characteristics of microtremors and the strong shaking of earthquakes. However, many micro zonation studies in Indonesia, including in Lombok, still rely heavily on microtremor data to determine parameters. The f_0 and A_0 without validation or direct comparison with local earthquake data, the fundamental problem is the lack of quantitative comparative studies in Lombok, resulting in the HVSR microtremor method's empirically untested reliability in this region.

Therefore, this study aims to directly address these problems. The f_0 and A_0 parameters of the HVSR method were analyzed and compared using microtremor and earthquake data. The analysis was conducted at the same seven seismic stations on Lombok Island to ensure valid comparisons. This study aims to evaluate the extent to which the HVSR microtremor results can reliably represent the actual site characteristics in Lombok, a complex geological area. The results of this study are expected to provide a strong scientific basis for future seismic micro zonation practices, both in Lombok and in other areas with similar conditions.

2. Data

This study selected recorded data from seven permanent seismograph stations belonging to the BMKG on Lombok Island, namely stations with the codes BYLI, KLNI, KMNI, LTNI, PBLI, SLBFM, and WLTFM. The seismographs at the permanent BMKG stations on Lombok Island are broadband seismographs. At the BYLI and KLNI stations, the sensors exhibit an equivalent frequency range from 0.0083 – 100 Hz, thus facilitating the detection of a comprehensive spectrum of seismic frequencies covering both large and subtle vibrations KMNI, LTNI and PBLI shows a frequency range of 0.003 – 50 Hz and 0.0083 – 50 Hz, respectively. All the above-mentioned seismometers are classified as broadband instruments capable of detecting seismic waves across frequencies with considerable sensitivity, albeit with slight differences in their frequency ranges. The ground response can be modeled as a single-degree-of-freedom (SDOF) oscillator with a single resonance frequency, determined from the maximum resonance of the HVSR [8].

HVSR data processing often faces challenges from disturbances such as anthropogenic sources, wind noise, and instrument drift. Noise data collection is recommended to minimize the influence of anthropogenic sources and reduce the effects of noise. Wind noise and instrument drift effects can be reduced by applying a second-order Butterworth high-pass filter above 0.5 Hz. Signal data are usually separated into "noise" and "earthquake" segments, with each segment split into 40-second windows with 50% overlap for FFT calculations. The resulting spectrum is processed using a Band Pass Filter (BPF) with range frequency 0.1- 20 Hz [7], producing three spectra for the north-south (SNS), east-west (SEW), and vertical (SZ) components [8]. Ambient noise recording data from each accelerograph station was collected at night for a one-hour period. Night time data collection is expected to reduce vibrations caused by human and machine movements.

Meanwhile, BMKG recorded 59 earthquakes around Lombok, originating from various faults and subduction zones. The earthquake data ranged from 2018 to 2025, with magnitudes ranging from 4.2 to 7.6 and hypocenter depths ranging from 4 km to 624 km (Fig. 1). Supporting indicators are needed to address the variations in A_0 and f_0 values obtained from the earthquake data set used. Indicators used geological conditions from the geological map (Fig. 2).

3. Methodology

This study uses a Horizontal-to-Vertical Spectral Ratio (HVSR) approach utilizing two data sources: microtremor recordings and earthquake recordings. The purpose of using these two datasets is to evaluate the consistency of the site's dynamic response parameters derived from ambient vibration conditions and from actual earthquake events. The initial stage of the analysis begins by converting the seismic signal from time domain to frequency domain using the Fast Fourier Transform (FFT). This transformation is necessary to obtain the amplitude spectra of the horizontal and vertical vibration.

Once the frequency spectrum is obtained, HVSR curves are calculated for the microtremor and earthquake datasets by comparing the ratio of the horizontal spectrum to the vertical spectrum. To ensure the stability of the HVSR curve peak (A_0) and

the estimated dominant frequency (f_0) that can be interpreted physically, a validation process was carried out based on the SESAME (2004) criteria. Next, a statistical analysis was performed to evaluate the relationship between ambient microtremor noise and earthquake source characteristics.

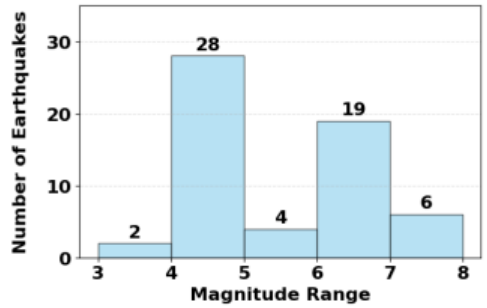

(a)

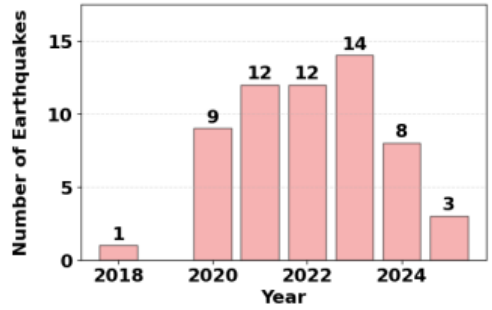

(b)

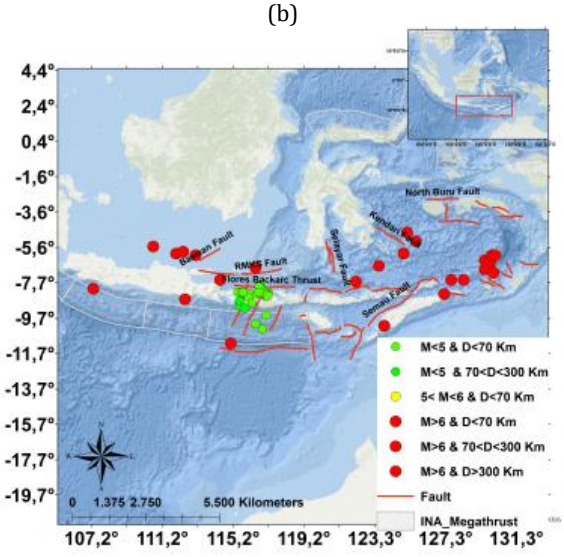

(c)

Fig. 1: (a) Distribution of earthquake magnitude, (b) Number of earthquakes, (c) Map distribution of earthquake locations the one used in this study.

The relationship between A_0 and f_0 with magnitude, distance, and azimuth was evaluated using scatterplots and linear regression, while the strength of the linear relationship was quantified using the Pearson correlation coefficient (R). Furthermore, the consistency between the HVSR parameters derived from microtremors and earthquakes was tested through a direct comparison approach using a fit reference line ($y = x$). Deviations from the ideal fit were evaluated using tolerance limits ($\pm\sigma$) and 95% confidence intervals (CI). This methodological suite allows for a comprehensive evaluation of the stability of site response parameters, while strengthening the interpretation that f_0 and A_0 characteristics are primarily controlled by local geological conditions, rather than solely influenced by variations in earthquake sources or distance between events (Fig. 3).

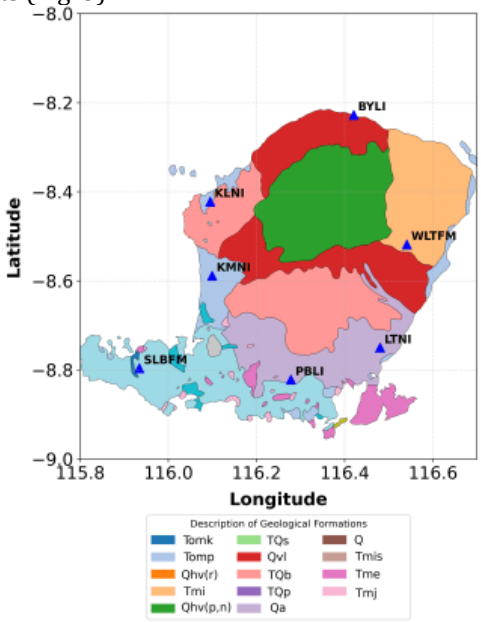

Fig. 2: Map of station distribution in relation to Lombok geology

3.1. HVSR Method

The ambient noise and earthquake recording signals obtained at seven permanent stations belonging to the BMKG are still in the time and velocity (cm/s) domain. These signals require transformation from the time domain to the frequency domain using the Fast Fourier Transform (FFT) calculation technique. The general FFT equation is as follows,

$$X[k] = \sum_{n=0}^{n-1} x[n] e^{\frac{-i2\pi nk}{N}} \quad (1)$$

with: $x[n]$ is the time domain signal, N is the number of samples in the signal, $X[k]$ is the frequency domain signal (k = 0.1, … N-1), the complex unit. The results of applying this FFT method will describe the velocity spectrum.

The HVSR method was introduced by [1], where the amplitude of the horizontal component of the Fourier is compared with the vertical component of a sensor on the surface. The resulting H/V ratio is the ratio between the horizontal component and the vertical component from the FFT results. When the measurement on the surface already represents the measurement in the bedrock, the amplitude of the vertical direction wave in the bedrock does not experience significant changes when passing through the sediment layer. So that it can be assumed as the one value, but it does not apply to the amplitude of the horizontal component, as shown below:

$$HVSR_s = \frac{Hs}{Vs} \quad (2)$$

Hs is the horizontal Fourier spectrum recording on the surface and Vs is the vertical Fourier spectrum recording on the surface. The Fourier spectrum ratio (H/V) is 1 in the bedrock because horizontal and vertical waves propagate evenly in the bedrock:

$$HVSR_b = \frac{Hb}{Vb} = 1 \quad (3)$$

where H_b and V_b represent the spectral horizontal and vertical vibrations of the incoming bedrock. Seismic waves propagate from the bedrock to the surface where the vertical component does not increase so that the vertical transfer function (TF_V) approaches 1.

$$TF_V = \frac{Vs}{Vb} \approx 1 \quad (4)$$

So, the transfer function of the horizontal component is:

$$TF_H = \frac{Hs}{Hb} \quad (5)$$

Based on the formula above, the following relationship is obtained:

$$HVSR_S = TF_H \, x \, HVSR_b \, x \frac{1}{TF_v} \quad (6)$$

From the equation above, $HVSR_S$ and TF_H can be expressed as the same on the surface, in other words, $HVSR_S$ can be used as a transfer function.

$$HVSR_s = \frac{Hs}{Vs} = \frac{Hs}{Hb} x \frac{Vb}{Vs} x \frac{Hb}{Vb} = \frac{Hs}{Vs} \quad (7)$$

There are similar empirical results between the transfer function (TF) and HVSR, related to the resonance frequency (f_0) at the location. Then the form of the equation becomes:

$$HVSR_S \approx TF_H \quad (8)$$

$HVSR_b$ tends to be uniform for ambient noise on average, which is determined by the width of the windowed S-wave recording when depending on the earthquake focal mechanism. Therefore, because TF_H and TF_V independent of the source, $HVSR_S$ *will* also depend on the source mechanism.

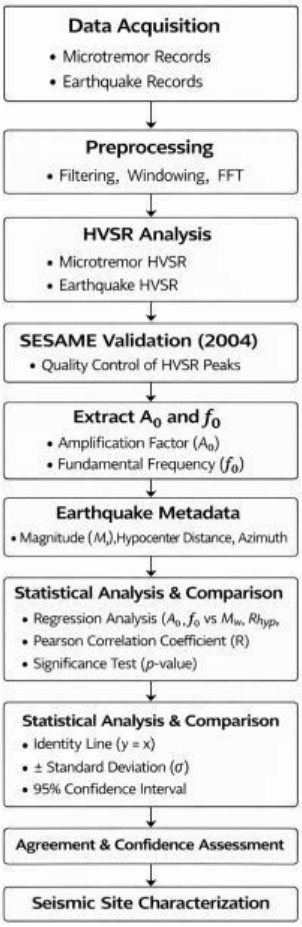

Fig. 3: Flow diagram of data processing in this study.

The location effect of ground motion can always be related to the location-reference spectral ratio (*SSR*) of the horizontal component of the S-wave motion recorded on the surface of the soil and rocks.

Application of horizontal transfer functions using S-waves attributed to resonance phenomena associated with shear waves propagating through the ground. Compared with traditional spectral ratio methods, the *H/V* spectral ratio obtained through *HVSR* can be used as an index to reflect site nonlinearity. The dominant frequencies measured by this method provide essential information about the thickness of the surface sediment layer (Fig. 4).

Amplification, which is the increase in the level of ground shaking caused by rock impedance contrast and the accumulation of wave propagation in the basin geometry, is greater when the surface rock is soft and the sediment is thick. The impact of an earthquake is quantified in terms of the transfer function of vertically propagating, horizontally polarized shear (*SH*) waves. For a simple case, such as a uniform viscoelastic layer of sediment with thickness (h) and shear wave velocity (V_s) overlying a viscoelastic bedrock, the resonance frequency (f_n) of the SH wave transfer function is calculated by the equation:

$$f_{n=(2n+1)} \frac{V_s}{4h}, (n = 0, 1, 2, ...) \quad (9)$$

Based on empirical research involving measurements of vertical and shear wave profiles down to bedrock, as well as recordings of seismic events at small strains, the lowest frequency peak of the HVSR can be related to the fundamental mode resonance frequency (f_0) of the soil layer above the elastic half-space due to shear wave propagation [11]-[13].

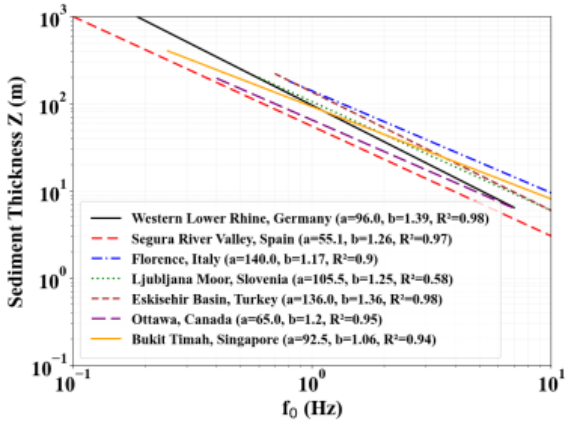

Fig. 4: Relationship between sediment thickness and natural frequency (f_0) (modified from [3]).

3.2. Statistical Analysis

Statistical analysis is needed to quantitatively compare parameters, namely resonance frequency (f_0) and amplification factor (A_0) generated from microtremor and earthquake data recorded at seven seismic stations on Lombok Island. It also to evaluate the HVSR method in seismic risk mapping in areas with complex geological conditions [1], [2], [7]. By knowing how strong the relationship between microtremor and earthquake data is, it can be used as

a basis for more accurate mapping model. The relationship between earthquake-derived parameters (x) and microtremor-derived parameters (y) was first examined using a simple linear regression model to identify general trends and potential systematic biases. The regression formulation follows the classical ordinary least-squares (OLS) approach [14], [15] :

$$y_i = ax_i + b + \varepsilon_i \quad (10)$$

where a is the slope, b is the intercept, and ε_i represents the residual error for each observation i. The regression coefficients were estimated using the ordinary least-squares approach by minimizing the sum of squared residuals [16]:

$$\frac{Min}{a,b} = \sum_{i=1}^{n}(y_i - (ax_i + b))2 \quad (11)$$

with the slope and intercept given by [15] :

$$a = \frac{\sum_{i=1}^{n}((x_i-\bar{x})\,(y_i-\bar{y}))}{\sum_{i=1}^{n}((x_i-\bar{x}))^2} \quad (12)$$

$$b = \bar{y} - a\,\bar{x} \quad (13)$$

Statistical methods used include correlation analysis using Pearson Correlation (r) [17]:

$$r = \sum_{n=1}^{\infty} \frac{n\sum xy - \sum x \sum y}{\sqrt{(n\sum x^2 - (\sum x)^2(n\sum y^2 - (\sum y)^2)}} \quad (9)$$

where N is the number of data, x and y are the two variables being tested, $\sum xy$ is the sum of the results of multiplying each pair of data x and y, $\sum x$ and $\sum y$ are the sum of the values of x and y, $\sum x^2$ and $\sum y^2$ are the sum of the squares of the values of x and y.

Theoretically, for low impedance contrasts, the maximum singularity of Rayleigh waves typically occurs within a frequency range of 0.5 to 1.5 times the fundamental frequency, which supports the interpretation of HVSR peaks as primary indicators of site resonance [9]. Building upon this theoretical framework, the maximum and minimum standard deviation limits of the resonance frequency (f_0) and amplification factor (A_0) distributions are employed to assess the extent of deviations (outliers). These deviations are calculated as [16]):

$$\varepsilon_i = (y_i - \hat{y}_i) \quad (15)$$

and the predicted value is:

$$\hat{y}_i = ax_i + b \quad (16)$$

The dispersion of residuals was quantified using the standard error of regression [16]:

$$\sigma = \sqrt{\frac{1}{n-2}\sum_{i=1}^{n}(y_i - \hat{y}_i)^2} \quad (17)$$

Thus, the prediction interval can be expressed as:

$$\hat{y}_i = ax_i + b \pm \sigma \quad (18)$$

where $\hat{y}_i$ = estimated value by the model. We include the addition of uncertainty estimates or confidence intervals 95% to further strengthen the robustnes of the analysis [18]. Then the equation :

$$\hat{y}_i = ax_i + b \pm 1.96\,\sigma \quad (19)$$

where 1.96 is the critical value of the standard normal distribution corresponding to a 95% confidence level, i.e.

$$P(|Z| \leq 1.96) = 0.95 \quad (20)$$

The analytical framework for HVSR parameters employs a dual-scaling approach to effectively decouple distinct physical characteristics from statistical behaviors. The amplification factor (A_0) is represented on a linear scale to provide a direct, uncompressed assessment of the soil's resonance magnitude, which is critical for quantifying the absolute energy excitation relevant to engineering design [19], [20]. Conversely, the resonance frequency (f_0) is evaluated using a log-log approach to reveal power-law distributions and exponential transitions that characterize wide-scale seismic datasets [21]. This logarithmic framework is essential for isolating low-level ambient noise from authentic seismic signals and facilitating rigorous outlier removal, thereby ensuring the reliability of the site response estimates [22], [23].

To validate the consistency between noise-derived and earthquake-derived parameters, an identity line (y = x) is utilized as a benchmark for perfect correlation. This 1:1 reference serves as a diagnostic tool to identify systematic biases, the closer the data clusters to this line, the higher the portability of microtremor data as a proxy for actual seismic response [9]. Furthermore, the inclusion of 95% uncertainty bands, which offer broader statistical coverage than standar deviation limits, allows for a clear distinction between typical variability and significant estimation errors, reinforcing the robustness of the comparative analysis. Data points that fall outside this envelope are considered anomalous deviations that can be caused by variability between earthquake events, nonlinear site response, or local subsurface heterogeneity [2], [7].

4. Results and Discussion

This study analyzes f_0 and A_0 using the HVSR method by utilizing microtremor and earthquake data from BMKG permanent stations, namely: SLBFM, BYLI, WLTFM, LTNI, KLNI, PBLI, and KMNI on Lombok Island. This method can detect dominant frequencies well which are closely related to sediment depth and thickness [24], [25] as well as to assess location effects [26]. This study reveals the complex dynamics of dependence between amplification (A_0) and fundamental frequency (f_0) on earthquake source parameters, namely epicentral distance, magnitude, and azimuth.

Lombok Island seismic stations that fundamentally reflect the influence of Quaternary volcanic geology from the Samalas eruption of 1257 AD [27], where shallow trachyandesite deposits (100–150 MPa) create lithological non-uniformities that affect the stability of the site response, with f_0 as

an indicator of the site's inherent geology that is not affected by variations in earthquake sources. The results of this analysis are then used to understand the consistency of f_0 and A_0 parameters against the influence of magnitude, distance, and azimuth, as well as how much correlation these parameters have from earthquake recordings and ambient noise. Initial hypothesis in this study, and A_0 have only a small influence on magnitude, distance, and azimuth, which can be seen from the correlation values and slope lines produced in the regression analysis. Therefore, the f_0 and A_0 results obtained from microzonation measurements for earthquake hazard mapping can reflect the actual seismic hazard conditions in the area. These results are also expected to answer some doubts regarding the results of microzonation research for earthquake hazard mitigation in the future.

4.1. Earthquake Signals, Noise Signals, and HVSR Curves

The initial investigation was conducted by collecting data from two dissimilar categories of seismic signals, namely microtremor (ambient noise) and earthquake signals. Both data were recorded by seven seismic stations operated by BMKG on Lombok Island: BYL, KLNI, KMNI, LTNI, PBLI, SLBFM, and WLTFM shown in Fig. 5. Both signal categories function well to generate and are used for comparison of HVSR curves with the aim of assessing the consistency of the site response. The analysis of the microtremor signals was conducted using the Microtremor Horizontal-to-Vertical Spectral Ratio (MHVSR) methodology, which summarizes local resonance attributes arising from the dominance of surface waves, particularly Rayleigh waves in a stationary, non-seismic environment [13], [27].

In contrast, earthquake signals are studied through Earthquake Horizontal-to-Vertical Spectral Ratio (EHVSR) which utilizes original seismic wave recordings to describe the dynamic response of sedimentary layers to excitation caused by earthquake waves [28], [29]. The comparison between these two spectral curves provides an empirical basis for validating the MHVSR results. If the dominant frequency (f_o) and maximum amplitude (A_0) derived from MHVSR show agreement with the findings from EHVSR, it can be concluded that the resonance characteristics captured by ambient noise activity have a physical equivalent to the actual response to seismic wave activity [29], [30].

Conversely, any differences manifested between the two could indicate the effects of subsurface heterogeneity, the direction of incident waves, or the relative contribution of body wave energy in relation to surface waves [9]. Consequently, a comparative analysis between MHVSR and EHVSR emerges as an important initial step in confirming the interpretation of location effects at each observation station. This methodological approach has also been widely used in microzonation research and seismic site characterization in various tectonically active regions, including Indonesia [31], [32]. The signal data processing using the HVSR method uses the open-source software geopsy, python, and obspy. The initial signal will undergo data classification, windowing using a sampling range of 30–50 seconds, and conversion from the time domain to the frequency domain using the FFT.

To ensure that the site parameters (f_0 and A_0) represent local geological conditions rather than earthquake source effects, we statistically evaluated their relationship with magnitude, distance, and azimuth (Fig. 6 and 7).

Regression trends were modeled using ordinary least-squares (Eq. 12), with coefficients estimated following Eq. 13–15. The strength of these associations was quantified via Pearson correlation coefficients (Eq. 16), while data consistency was tested using residual dispersion and agreement limits (Eq. 17–20). Finally, a conservative 95% uncertainty envelope was constructed (Eq. 21–22) to identify statistically significant deviations, thereby confirming the reliability of the derived HVSR parameters for seismic hazard analysis.

4.2. BYLI Seismic Station

BYLI station according to the geological map is located in the Quaternary volcanic breccia which is lithologically composed by andesitic to basalt fragments, porous, thick-layered, and highly permeable, the result of plinian deposits from the eruption of Mount Samalas [33]. With a microtremor f_0 value of 0.86 Hz associated with a thick sedimentary layer resulting in a moderate-low seismic impedance contrast between the surface and underlying layers. The distribution of the earthquake f_0 values shows a very weak positive dependence on distance (slope = 0, r = 0.038) shown on Fig. 6. Where the value (f_0) of the earthquake recorded at the station tends to have a slight increase at distances > 600 km associated with the dominance of surface waves in far-field source propagation.

In this condition, the source wave frequency close to the microtremor site f_0 (0.86 Hz) can trigger partial resonance, especially when the wave energy is trapped and amplified by a thick and highly porous breccia layer. This phenomenon shows that the interaction between long-period Rayleigh waves and volcanic subsurface structures can amplify the amplitude without significantly changing the f_0 value [33].

Meanwhile, A_0 to magnitude shows a low inverse relationship (slope = -0.06, r = -0.161). The decrease in A_0 begins at magnitudes >6.5 due to resonance if the earthquake frequency approaches the f_0 of microtremor (0.86 Hz) a nonlinear resonance will occur where an increase in dynamic stress causes a decrease in the effective shear modulus and an increase in the internal damping of the material.

As a result, A_0 decreases, even though f_0 remains constant. This is consistent with the Rayleigh wave ellipticity model which shows that A_0 at low frequencies is extremely sensitive to lateral non-uniformity and nonlinear damping [12].

Figure 6 shows the relationship between A_0 and f_0 and azimuth has a minor effect. The A_0 azimuth value has a slope close to zero with a low correlation (0.172), while the stable f_0 azimuth (r = 0.045) reflects a relatively weak anisotropic northern volcanic path of propagation, where the azimuth passing through the thick magma and sediment areas around Mount Rinjani causes attenuation of A_0, due to wave scattering in the thick volcanic layer that absorbs

earthquake wave energy, especially when the wave direction passes through the sedimentary basin and magma chamber [34].

A) Microtremor Recording Data

B) Earthquake Recording Data

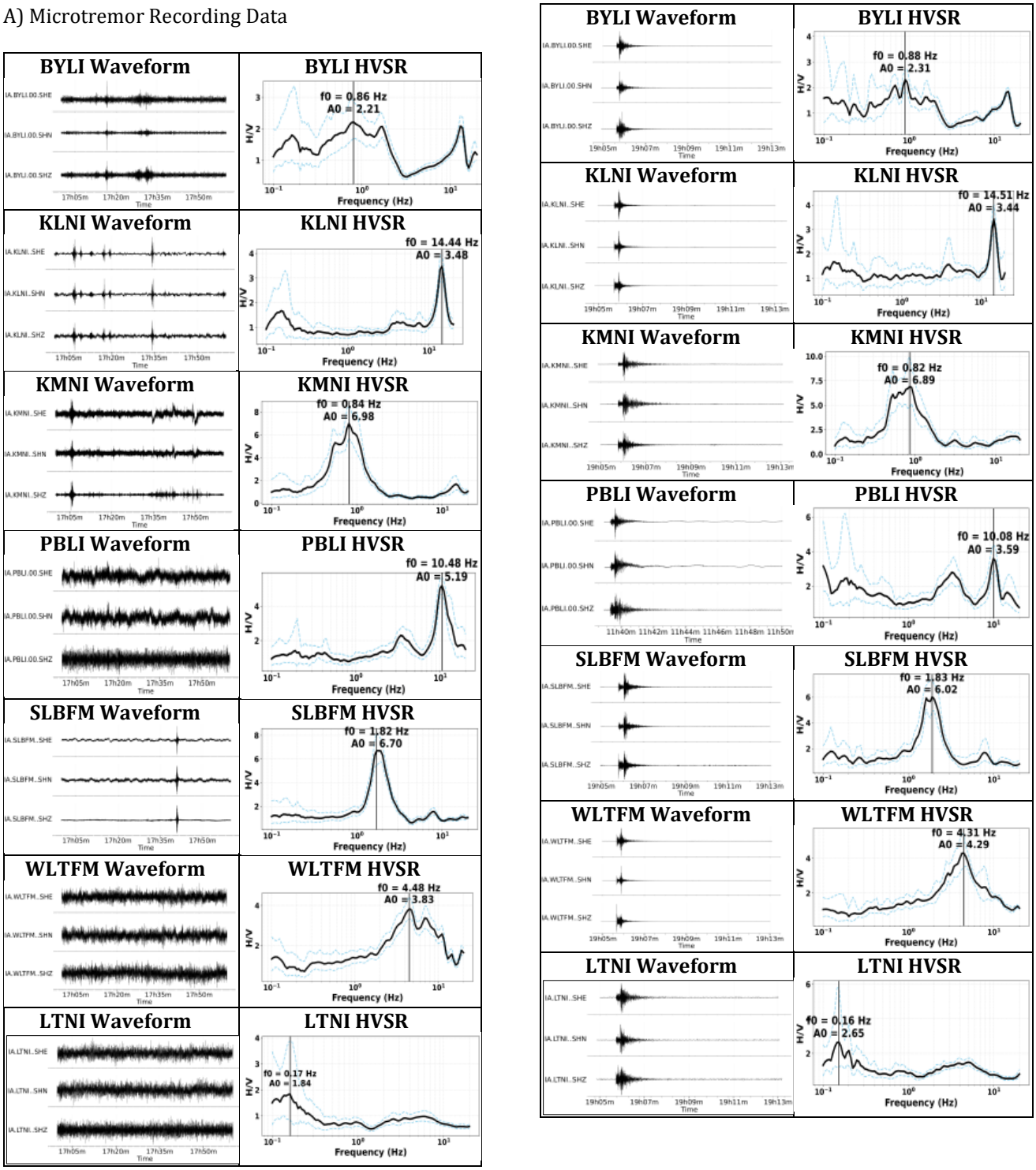

Fig. 5: (A). Microtremor signal for each station and the results of f_0 and A_0, (B). Earthquake signal for each station and the results of f_0 and A_0.

In general, the orientation of the propagation path does not significantly affect the site resonance, indicating lateral homogenenity in the volcanic breccia layer beneath the station. The f_0 value, however, remains stable across all variables ($r<0.05$), consistent with the low microtremor f_0 reflecting the constant impedance contrast of the thick breccia, where HVSR effectively distinguishes the inherent resonance of the site geology without source influence, making f_0 a representation of the site geology condition that is unaffected by anything, including earthquake source variations [24]. Here, the geology of the volcanic breccia explains the more prominent A_0 variation in near-field earthquakes, where near-field body waves trigger resonance, while far-field earthquakes exhibit a stable response. The stability of the f_0 value as an inherent geological property of the site is consistent with the single degree of freedom (SDOF) oscillator approach.

A simple model that considers the site as a single oscillator with a single resonance frequency (f_0) as the center frequency remains linear and reflects the underground structure without external distortion [14].

4.3. KLNI Seismic Station

KLNI Station is located above Quaternary volcaniclastic breccia with the f_0 value of the microtremor having a high value of 14.4 Hz. From Fig. 7 shows that A_0 increases against a relatively small magnitude (slope = 0.13; r = 0.333) and against a relatively constant distance (slope = 0 ; r = 0.189), while the distribution of earthquake f_0 tends to be constant against magnitude (slope = -0.01; r = -0.046) and distance (slope = 0; r = 0.023). Where the A_0 trend experiences a slight increase starting at a magnitude > 4.5 indicates linear amplification in stiff rocks, where resonance occurs at high frequencies due to a thin sedimentary layer. Variations in A_0 values are more prominent in nearby earthquakes due to the non-linear effects of the subsurface soil medium, while variations in earthquake f_0 values remain constant where the wavefield is stable as an indicator of the inherent geology of the site [12]. The low correlation of f_0 with magnitude and distance indicates that the dominant site frequency is not affected by these two parameters [34].

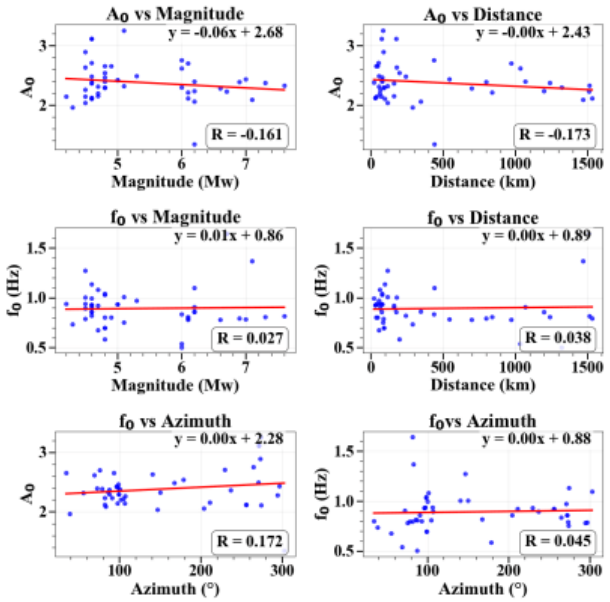

Fig. 6 : Correlation results of f_0 and A_0 at BYLI seismic station on magnitude, distance, and azimuth.

The distribution of A_0 values against azimuth shows a small negative slope (slope = 0; r = -0.078), indicating a weak and isotropic relationship between amplification and wave arrival direction. The dominant amplitude originates from the east of the station, where the eastern azimuthal path passes through thin sediment causing minimal attenuation, in contrast to the western path which passes through a sedimentary basin and thus experiences greater attenuation. Mark f_0 shows a stable distribution (slope ≈ 0; r = -0.003) with a good agreement between f_0 microtremor and f_0 earthquake, both showing a high dominant frequency indicating a thin sediment thickness beneath the station.

This condition is consistent with the character of heterogeneous volcaniclastic breccia, where high impedance contrast in shallow layers limits resonance and makes f_0 an inherent geological property of the site that is not affected by source variations [33]. The distribution of A_0 also shows a dominance at high frequencies, with an isotropic azimuthal distribution. This pattern indicates the homogeneity of the geological structure around the KLNI station, where the site response is more influenced by the proximity of shallow bedrock than by the direction of earthquake wave arrival. This finding is consistent with the results of [1] and [25] which show that areas with shallow bedrock produce high f_0 values due to the large impedance contrast between thin sediment layers and bedrock.

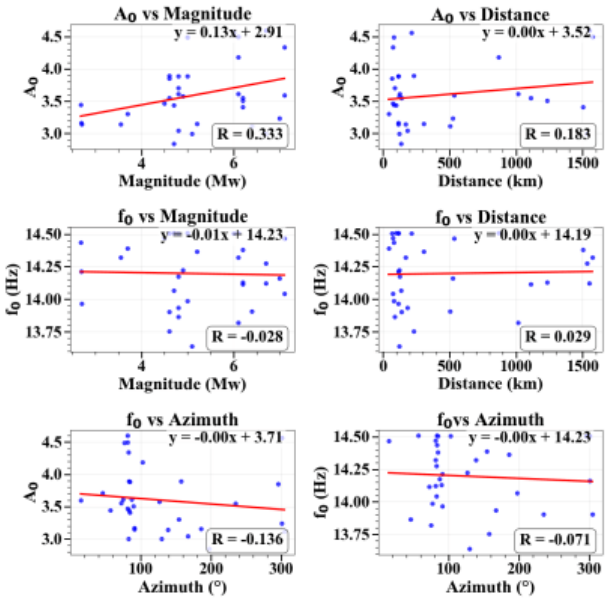

Fig. 7. Correlation results of f_0 and A_0 at the KLNI seismic station on magnitude, distance, and azimuth.

4.4. KMNI Seismic Station

KMNI Station is located on Quaternary unstructured alluvial sediments with f_0 microtremor 0.836 Hz. Based on the analysis results shown on Fig. 8, A_0 shows a moderate negative dependence on distance (r = -0.378) and magnitude (slope = -0.34; r = -0.314), indicating that amplification tends to decrease at distances >200 km and large earthquakes (M >5) due to energy attenuation and non-linearity of soft soil. The increase in dynamic strain in large earthquakes causes a decrease in the soil shear modulus and an increase in viscoelastic damping, so that the A_0 amplitude decreases at the dominant site frequency [35].

The high variation of A_0 at distances <400 km and magnitudes <5.5 indicates the presence of local site resonance due to the source frequency ($f_{earthquake}$) which is close to the natural frequency of the site (f_{site} = 0.84 Hz). Under these conditions, near-field body waves still carry high energy and medium frequencies, strengthening the elastic soil response in the highly porous sedimentary layer. Meanwhile, A_0 with respect to azimuth (slope = -0.01; r = 0.127) shows weak directional anisotropy, where the southward direction passing through the thick alluvial sedimentary basin shows amplitude attenuation due to the absorption of wave energy by the soft layer.

In contrast, the f_0 distribution of the earthquake data shows high stability (slope = 0; r < 0.20) across magnitude, distance, and azimuth. The low f_0 value of 0.84 Hz reflects the significant thickness of alluvial sediments, which produces a low resonance frequency typical of soft soils. The similarity of f_0 values between the microtremor and earthquake results indicates that resonance is dominated by

vertical impedance contrast, rather than by variations in the source or direction of the waves. This finding is consistent with the research of [24] who reported that alluvial basins tend to produce low f_0 values due to sediment thickness. Low-frequency surface waves dominate and cause f_0 to remain constant as an indicator of the site's inherent geology [3], [34]. This confirms that alluvial sediment thickness plays a dominant role in determining the fundamental frequency (f_0) at the KMNI site.

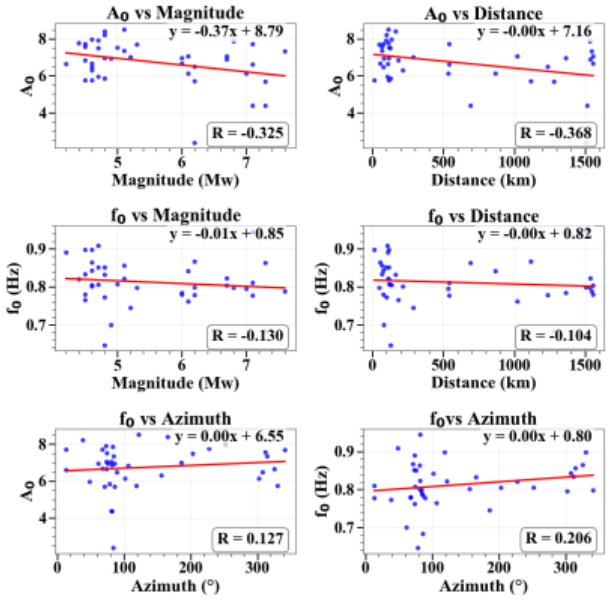

Fig. 8: Correlation results of f_0 and A_0 at the KMNI seismic station on magnitude, distance, and azimuth.

4.5. LTNI Seismic Station

The Station of LTNI is in the Quaternary tufaceous breccia unit with f_0 from microtremor data is low (0.175 Hz). According to geological history, this area is composed of thick and highly porous Samalas plinian tuff deposits, reflecting volcanic sediment layers resulting from large eruptions with strong vertical impedance contrasts [27]. Based on Fig. 9, the distribution of A_0 with distance shows a small negative slope (r = -0.165), indicating a tendency for a weak decrease in amplitude with increasing source distance. This trend indicates that body waves in propagation from far-field sources experience energy attenuation due to the large distance and energy-absorbing lithology properties, so that the resonance amplitude decreases slowly at distances > 500 km.

The relationship of A_0 with magnitude shows a weak negative slope (slope = -0.08; r = -0.189), indicating that amplification decreases with increasing earthquake magnitude (> 5.5). This indicates a weak nonlinear response in moderate to soft soils, where increased earthquake excitation causes a decrease in effective stiffness and an increase in viscoelastic damping, resulting in a decrease in peak amplification (A_0) at the site's dominant frequency. However, due to the low correlation (r < 0.2), this relationship is still indicative. The larger variations in A_0 at distances <500 km and for earthquakes with magnitudes <5.5 can be explained by several interrelated physical factors. At near-field distances, seismic waves still contain high-frequency components and direct wave energy that has not experienced much anelastic damping or scattering by medium heterogeneity.

This condition causes the wave amplitude arriving at the surface to be large, especially in soft sedimentary layers such as Quaternary tufaceous breccia. Because this layer has low impedance and high porosity, the incoming wave energy will be trapped and experience local resonance, resulting in high A_0 values. Furthermore, in small to moderate magnitude earthquakes (M < 5.5), the emitted earthquake energy is low, but the dominant frequency is higher than in large earthquakes. This high frequency is more easily resonated with the dominant frequency of the site (f_0 = 0.175 Hz) if there is a match in the low to medium frequency range. This partial resonance causes amplification (A_0), especially when the sediment layer is thick and flexible [9].

The distribution of A_0 with respect to azimuth is neutral (r = -0.034), indicating very weak directional anisotropy. Although the eastward direction of the station passes through a thick sedimentary layer and a volcanic basin that could theoretically reduce the amplification (A_0) due to the absorption of wave energy by the sedimentary basin, these data do not yet show a significant directional pattern.

Figure 9 shows that the distribution of f_0 values from earthquake data is relatively stable with respect to magnitude and azimuth (r = 0.004 and r = 0.048, respectively) with a very weak increase with distance (r = 0.111), consistent with the microtremor f_0 results which display a low dominant frequency of 0.18 Hz, associated with the presence of a thick sedimentary layer. This indicates that the resonance of the site is determined by the vertical impedance contrast between the thick tuff layer and the bedrock, not by source factors. However, in far-field earthquakes, the earthquake f_0 remains constant as an inherent geological characteristic of the site, in accordance with the HVSR principle which is able to capture subsurface impedance contrasts without being influenced by source variations [9], [36].

4.6. PBLI Seismic Station

PBLI Station is in the Quaternary tuff breccia unit with a microtremor f_0 of 10.48 Hz indicating shallow hard rock conditions with a thin sediment layer on the surface. Based on the analysis results (Fig. 10), the distribution of earthquake data shows a very weak positive relationship with distance (r = 0.101) and magnitude (slope = 0.20; r = 0.167). This slight increase indicates that A_0 increases slightly with increasing distance (>400 km) and magnitude (>5) due to the dominance of surface waves in far-field propagation which tend to be more effective in amplifying the response of hard ground at high frequencies. At short distances (<400 km) and small magnitudes (<5.5), the observed A0 variations are caused by interference between body waves and high-frequency resonances in the thin sediment layer.

The lithological conditions of heterogeneous tuff-breccia cause non-uniform energy reflection at the hard rock-sediment interface, resulting in small fluctuations in A_0. Meanwhile, the distribution of A_0 against the small correlation azimuth (r = 0.078) shows an isotropic pattern without a dominant direction, consistent with a homogeneous layer around the PBLI. These results indicate that the PBLI

site is rigid, with dominant amplification at high frequencies (>10 Hz) and little influence of the direction or distance of the source at that location.

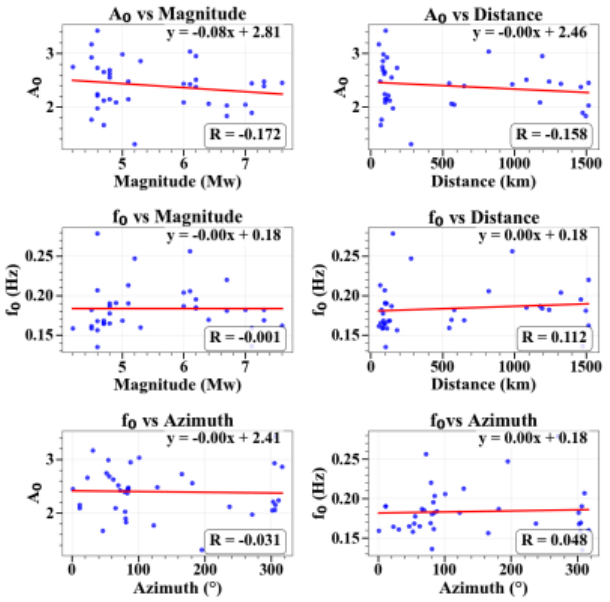

Fig. 9: The results of the correlation of f_0 and A_0 at the LTNI seismic station on magnitude, distance, and azimuth.

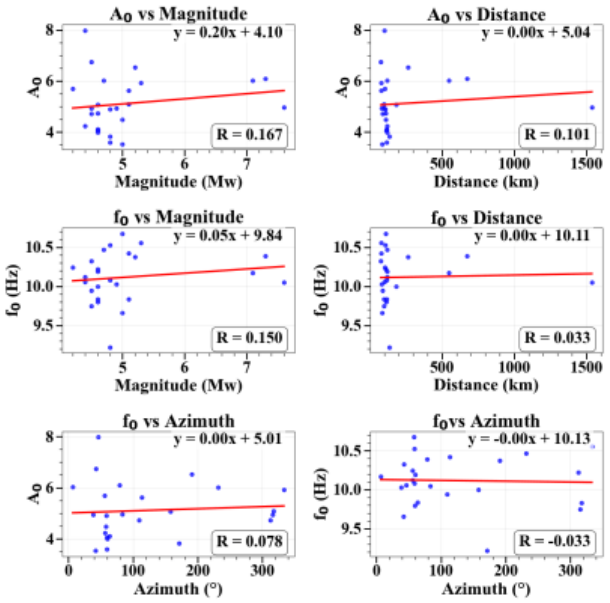

Fig. 10: Correlation results of f_0 and A_0 at the PBLI seismic station on magnitude, distance, and azimuth.

Figure 10 shows that the f_0 value shows high stability across all parameters (slope < 0.05; r < 0.15), reflecting the extremely high dominant frequency (f_0 = 10.48 Hz) typical of shallow hard rock/thin sediment sites. A very weak positive correlation with magnitude (r = 0.150) and distance (r = 0.033) indicates that f_0 only increases slightly with increasing source energy, but the effect is not significant. This stability confirms that the f_0 value in the PBLI is determined by the very thin sediment thickness and strong impedance contrast between the surface layer and the bedrock, rather than by variations in the earthquake source [9]. Thus, the f_0 value serves as an inherent geological parameter of the site, while small variations in A_0 reflect the elastic response of the hard layer to surface wave energy. This condition is in accordance with the recommendation of [9], that in sites with thin sediment and high impedance, the f_0 value tends to be constant and resonance is insignificant. In general, PBLI represents the characteristics of hard footing, high dominant frequency stability, and a seismic response dominated by low-amplitude high-frequency waves.

4.7. SLBFM Seismic Station

The SLBFM station is located on a Miocene sedimentary rock formation dominated by andesite-basaltic material. HVSR results show a microtremor f_0 of 1.82 Hz, representing thick sediment. Based on the analysis results (Fig. 11), A_0 shows a very weak negative linear regression slope with distance (r = -0.048) and magnitude (slope = -0.01; r = -0.0), indicating a weak but consistent relationship. This small correlation value indicates that the decrease in A_0 amplitude with distance and magnitude is minor, with a tendency to weaken at distances >800 km due to energy attenuation and the influence of vertical P waves in the far-field region that reduce A_0 at low frequencies [34]. The distribution of A_0 with respect to azimuth (r = 0.111) shows a weak directional influence, where the homogeneous sandstone-shale-limestone lithology indicates an isotropic response to wave propagation. Small variations in A_0 at distances <400 km and magnitudes <5.5 are caused by local resonances in surface waves (Rayleigh and Love) that are still strong in the near-field and the influence of elongated shallow basin morphology that increases the resonance amplitude at low frequencies [2], [37].

These conditions indicate that amplification in SLBFM is controlled by thick sediments and subsurface impedance contrasts, not by the earthquake source.

Figure 11 shows the f_0 distribution of earthquake data which has high stability across all parameters (r < 0.15), with weak positive correlations with distance (r = 0.146) and magnitude (r = 0.051), and a small negative correlation with azimuth (r = -0.254). This stability indicates that the f_0 value is an inherent geological characteristic of the site that is not affected by source variations. The low dominant frequency (1.82 Hz) indicates a thick sedimentary layer overlying hard volcanic rock, where vertical resonance is dominated by a strong impedance contrast between the soft sediment and the bedrock [9]. Potential resonance can occur when the earthquake source frequency ($f_{0\_earthquake}$) approaches the f_0 microtremor (1.82 Hz), especially in near-field earthquakes (<400 km), which causes an increase in A_0 without changing f_0.

This phenomenon is in line with the concept that f_0 is more stable to wavefield variations, while A_0 is more sensitive to energy dynamics and wave propagation direction [12]. Overall, SLBFM reflects a soft soil footprint with thick sediments, where low f_0 indicates potential for low-frequency amplification, while A_0 is relatively moderate due to damping effects and basin morphology that limit amplitude amplification in the near-field.

4.8. WLTFM Seismic Station

The WLTFM station is located on a Quaternary rhyolite lava unit with a microtremor f_0 value of 4.56 Hz, indicating medium-thickness sediment. Based on

the analysis results (Fig. 12), A_0 shows a low negative trend with respect to magnitude (slope = -0.16; r = -0.408) and with respect to distance (r = -0.258), indicating that amplification (A_0) decreases with increasing magnitude and source distance. A more pronounced decrease in A_0 values at magnitudes >5 indicates the non-linear damping effect of medium-soft soils, where increasing dynamic strain due to large earthquakes reduces the effective shear modulus and increases viscoelastic damping, causing peak amplification to decrease [34].

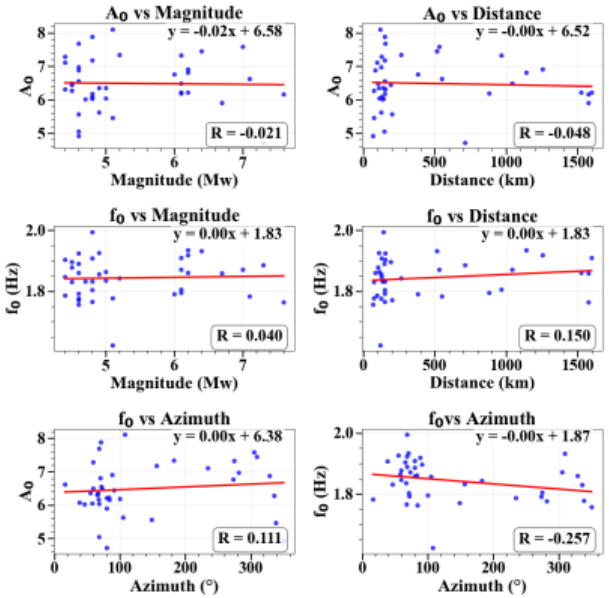

Fig. 11: Correlation results of f_0 and A_0 at the SLBFM seismic station on magnitude, distance, and azimuth.

Meanwhile, the decrease in A_0 values with distance reflects the attenuation of body wave energy and scattering in the far-field zone, especially after distances >1000 km, where surface waves dominate propagation. The distribution of earthquake A_0 values with respect to azimuth (r = 0.038) shows an isotropic relationship with no dominant direction, consistent with the homogeneous lithology of the lava flows resulting from the Samalas eruption. However, the direction passing through the thick lava zone and sedimentary basin at the summit of Rinjani may experience partial attenuation due to energy absorption by the highly porous volcanic layer. Overall, A_0 in WLTFM shows moderate sensitivity to magnitude and distance, but is stable with respect to direction, indicating that the effects of non-linearity and energy attenuation are more influential than azimuth anisotropy. Figure 12 shows the f_0 value has high stability for all parameters (r < 0.15), with a weak positive correlation with magnitude (r = 0.117) and distance (r = 0.139), and an exceedingly small negative correlation with azimuth (r = -0.043).

This trend indicates that the dominant frequency (f_0) is constant, reflecting the inherent resonance of the intermediate sedimentary layer above the lava bedrock. The high f_0 value (4.56 Hz) reflects the intermediate sedimentary thickness with a strong impedance contrast between the upper layer and the hard bedrock, so that resonance occurs at intermediate frequencies without wavefield distortion. Potential resonance can occur when the earthquake source frequency ($f_{earthquake}$) is close to the f_0 of the microtremor site (4.56 Hz), especially in nearby earthquakes (<400 km) which can increase the A_0 value without changing the f_0 value.

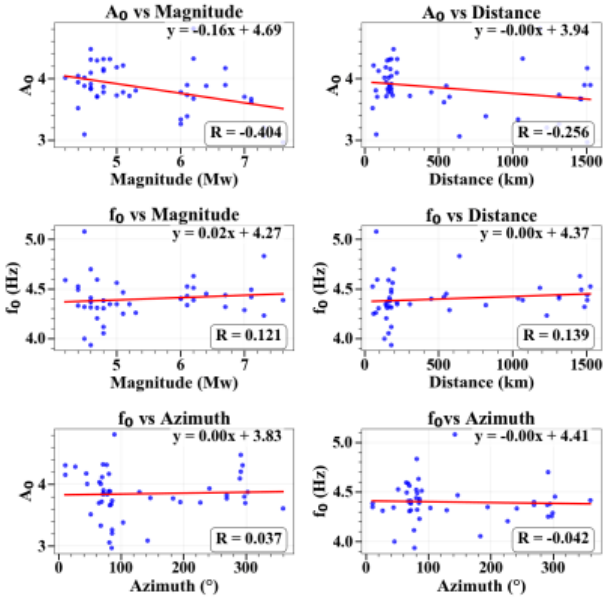

Fig. 12: Correlation results of f_0 and A_0 at WLTFM seismic station on magnitude, distance, and azimuth

The dense and homogeneous geological conditions of lava flows make f_0 very stable because the vertical impedance contrast dominates compared to the influence of the source or the direction of the wave arrival. In general, WLTFM represents a moderate volcanic footprint with a site response at mid-frequency, where A_0 is affected by soil non-linearity and distance attenuation, while f_0 remains a stable indicator of subsurface geology and is not affected by source variations.

4.9. Relationship between Resonance Frequency (f_0), Amplification (A_0), and Site Dynamics

Comparison of f_0 of microtremor and f_0 of earthquake at seven BMKG stations (BYLI, LTNI, KLNI, WLTFM, SLBFM, PBLI, and KMNI) shown in Fig. 13, almost perfect coherence (r = 0.9954) in logarithmic scale, with data distribution parallel to the line of equality (y = x). The dominant frequency range (f_0) of 0.175–14.44 Hz reflects the lithological variation from thick volcanic sediments to shallow hard footings. This result confirms that f_0 is source-independent and fully controlled by the vertical impedance contrast between sedimentary and bedrock layers, as explained by [30] and [31]. This stability indicates that MHVSR (microtremor) is able to replicate EHVSR (earthquake) results consistently, so it can be used to estimate subsurface resonance in areas with limited seismic data (Fig 13).

Despite the high correlation, some f_0 points show deviations from the positive logarithmic standard deviation limit, which is physically explained by Rayleigh wave singularities at low impedance contrasts [6]. When the impedance contrast is small, the fundamental Rayleigh mode produces an amplitude peak between 0.5 f_0 and 1.5 f_0, thus causing a pseudo-resonance. Stations LTNI and BYLI, with thick and porous tuff sediments, show negative deviations (minimum stdev) because resonance occurs at lower frequencies due to the trapping of

Rayleigh energy. In contrast, WLTFM and PBLI, which sit on lava and hard breccia, show positive deviations (maximum stdev) due to the contribution of body waves (P and S) that amplify the vertical component of the earthquake HVSR [32]. These results indicate that these small shifts are natural due to lateral heterogeneity and varying sediment thickness, rather than errors in the HVSR method. Thus, the distribution of f_0 around the maximum standard deviation at the seven Lombok station locations represents local non-uniformity of the subsurface structure, not analytical uncertainty.

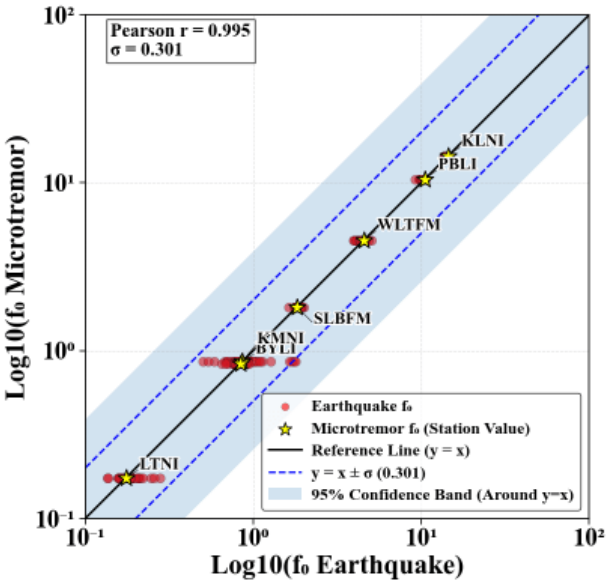

Fig. 13: Relationship between f_0 microtremors and f_0 earthquake.

Based on Fig. 13, the comparison of microtremor A_0 and earthquake A_0 shows a strong but imperfect correlation (r = 0.9232). The data are scattered around the y = x line, with microtremor A_0 slightly higher in soft soil sites (KMNI, SLBFM, LTNI) and lower in hard soil sites (PBLI, WLTFM). This condition indicates that A_0 is dynamic (dynamic-sensitive) and is affected by source energy, propagation distance, and soil non-linearity. These results are consistent with [34] and [12] who explained that body waves (P–S) from earthquakes reduce the H/V ratio at high frequencies (>2 f_0), while the HVSR of microtremors is dominated by fundamental Rayleigh waves, resulting in higher resonance amplitudes. Therefore, earthquake A_0 reflects actual amplification (dynamic gain), while microtremor A_0 reflects potential amplification (static gain).

Several A_0 points exceed the maximum standard deviation limit on a linear scale, especially in KMNI and SLBFM, where the microtremor A_0 is significantly higher than the earthquake A_0. This reflects the non-linear damping effect of soft soils, where increasing dynamic strain during large earthquakes decreases the soil shear modulus (G/G_0) and increases viscoelastic damping (ζ), resulting in a decrease in the actual resonance amplitude [9], [29]. In contrast, in WLTFM, PBLI, and KLNI, the earthquake A_0 is slightly higher than the microtremor A_0, indicating that high-frequency surface waves can amplify partial resonances in hard soils. Statistically, the deviation of A_0 beyond the maximum standard deviation indicates a local response controlled by damping and layer heterogeneity, rather than measurement error. At low impedance ratios, the Rayleigh resonance amplitude broadens and shifts from the actual f_0, resulting in a natural spread of A_0 between stations [27].

The relationship between f_0 and A_0 at seven stations demonstrates a close relationship between subsurface geological characteristics and the dynamic response of the soil to earthquake excitation. In general, f_0 describes the inherent properties of the sedimentary layer, while A_0 represents how strongly the layer amplifies vibrations at a given frequency. When the dominant frequency of the earthquake source approaches the natural frequency of the soil (f_0 earthquake ≈ f_0 microtremor), local resonance occurs and A_0 increases significantly, especially at sites with soft sediments such as KMNI, LTNI, SLBFM, and BYLI. Conversely, at hard sites such as PBLI and WLTFM, the source frequency is generally far from f_0 so that resonance does not form, resulting in a relatively small and stable A_0. This relationship illustrates that the closely aligned the earthquake energy is with the natural frequency of the soil, the greater the potential for amplification, whereas under conditions of high damping or frequency mismatch, the vibration amplitude will be naturally damped.

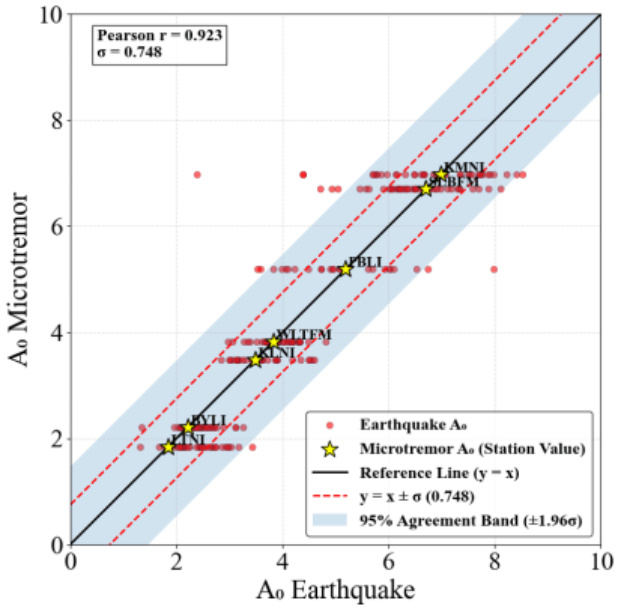

Fig. 14: Relationship between A_0 microtremor and A_0 earthquake.

The correlation between these parameters also indicates the influence of viscoelastic damping on soil response. In soft soils with large impedance contrasts, wave energy tends to be trapped longer in the sediment layer, increasing the surface amplitude and slowing energy dissipation. Conversely, in hard sites with high impedance and thin layers, most of the energy is immediately transferred to the bedrock, resulting in a weak and rapidly damped resonance response. This phenomenon is consistent with the results of [9] and [3], which showed that the maximum HVSR amplitude (A_0) increases in low-damping soils and decreases with increasing damping due to nonlinear deformation during large earthquakes. Thus, the combination of f_0 and A_0 can be used to assess the dynamic sensitivity of each site, i.e., how easily the soil layer resonates to incoming earthquake waves.

Integration of f_0 and A_0 results from seven Lombok stations shows that the HVSR microtremor (MHVSR) method is not only able to identify the dominant ground frequency resonance but also describes the actual amplification capacity during an earthquake. A stable f_0 value makes this method reliable for mapping subsurface structures and sedimentary layer boundaries, while a more variable A_0 provides an overview of the potential vibration amplification due to local dynamic conditions. Variations in amplitude around the standard deviation limits reflect the natural diversity of impedance contrasts, lateral heterogeneities, and damping levels, which according to [6] are a physical consequence of the Rayleigh singularity where the maximum resonance does not always occur exactly at the fundamental frequency, but can shift around 0.5 to 1.5 times f_0.

This distribution pattern is important in the context of microzonation and BMKG early action, because it shows the natural uncertainty limits of site response that must be considered in the ShakeMap system and earthquake hazard maps. Sites with large deviations (e.g., KMNI and LTNI) reflect high amplification areas that require more attention in mitigation, while sites with small deviations (e.g., PBLI and WLTFM) serve as stable references for model calibration. By understanding the relationship between f_0 and A_0, prompt action systems based on geophysical information can be made more responsive and accurate, because they are able to anticipate local resonance behavior before major shocks occur.

5. Conclusion

This study shows that the dominant frequency parameters (f_0) and amplification factors (A_0) of microtremor measurements (MHVSR) have an extremely high level of agreement with the measurement results from actual earthquake data (EHVSR) at seven BMKG stations on Lombok Island. The strong correlation between MHVSR and EHVSR from parameter f_0 ($r = 0.9954$, $\sigma = \pm 0.301$) and A_0 ($r = 0.9232$, $\sigma = \pm 0.748$), proves that the results of HVSR-based seismic microzonation can accurately represent the dynamic response of the ground when an actual earthquake occurs.

The consistent f_0 values across all stations confirm that the dominant ground frequency is a structure controlled geological characteristic determined by the vertical impedance contrast and sedimentary layer thickness and is not affected by earthquake source parameters such as magnitude, distance, or wave direction. In contrast, the more fluctuating A_0 variations reflect a source-controlled dynamic response due to damping effects, soil nonlinearity, and sediment heterogeneity. The small difference between microtremor A_0 and earthquake A_0 is a natural consequence of viscoelastic damping mechanisms and Rayleigh singularities.

Thus, the results of this study empirically address doubts about the accuracy of earthquake microzonation data. The f_0 and A_0 values from microtremor measurements are proven to be representative of real conditions during earthquakes and can be used as valid parameters for support the development of an adaptive, data-driven disaster mitigation system based on measurable scientific principles.

References

[1] Y. Nakamura, "A method for dynamic characteristics estimation of subsurface using microtremor on the ground surface", Quarterly Report of Railway Technical Research, 30, 25–33,(1989). https://www.sdr.co.jp/papers/hv_1989.pdf

[2] Bard, Pierre-Yves. Microtremor measurements: A tool for site effect estimation?. Conference: Second International Symposium on the Effects of Surface Geology on seismic motion at: Yokohama, Japan. Irikura, Kudo, Okada & Sasatani, (eds), Balkema 1999, Vol. 3, 1251-1279. (1998).

[3] S. Molnar, A. Sirohey, J. Assaf, P. Y. Bard, S. Castellaro, C. Cornou, B. Cox, Guillier, B., Hassani, B., Kawase, H., Matsushima, S., Sánchez-Sesma, F.J., and Yong, A., "A review of the microtremor horizontal-to-vertical spectral ratio (MHVSR) method", Journal of Seismology, 26(3), 653–685, (2022). DOI: 10.1007/s10950-021-10062-9.

[4] S. Stanko, S. Markušić, M. Gazdek, V. Sanković, I. Slukan and I. Ivančić, "Assessment of the seismic site amplification in the City of Ivanec (NW Part of Croatia) using the microtremor HVSR method and equivalent-linear site response analysis", Geosciences, 9(7), 312, (2019). DOI: 10.3390/geosciences9070312.

[5] P. G. d. Q. Iñárritu, N. Šipčić, L. G. Alvarez-Sanchez, M. Kohrangi and P. Bazzurro, "A closer look at hazard-consistent ground motion record selection for building-specific risk assessment: Effect of soil characteristics and accelerograms' scaling", Earthquake Spectra, 39(3), 1683–1720, (2023). DOI: 10.1177/87552930231174950.

[6] S. Bonnefoy-Claudet, A. Köhler, C. Cornou, M. Wathelet and P.-Y. Bard, "Effects of Love waves on microtremor H/V ratio", Bulletin of the Seismological Society of America, 98(1), 288–300, (2008). DOI: 10.1785/0120070063.

[7] SESAME Project, "Guidelines for the implementation of the H/V spectral ratio technique on ambient vibrations measurements, processing and interpretation", (2004). https://doi.org/10.1785/BSSA0840051350.

[8] G. Triantafyllidis, N. Theodulidis and E. Kirtas, "Seismic site effects in Greece: A comparison of microtremor and earthquake data", Journal of Seismology, 3(1), 63–74, (1999). DOI: 10.1023/A:1009841830605.

[9] Y. Xu and S. Wang, "Review and application of the H/V spectral ratio technique in site effect studies", Earthquake Engineering and Engineering Vibration, 20(4), 845–861, (2021). DOI: 10.1007/s11803-021-2057-3.

[10] C. Zhu, D. P. Thambiratnam, C. Gallage, N. Udawatta, "Reliability of HVSR-derived site response parameters: Comparison with empirical transfer functions and numerical modeling", Soil Dynamics and Earthquake Engineering, 138, 106315, (2020). DOI: 10.1016/j.soildyn.2020.106315.

[11] W. W. Wollery and R. Street, "3D near-surface soil response from H/V ambient-noise ratios",

Soil Dynamics and Earthquake Engineering, 22(9–12), 865–876, (2002). DOI: 10.1016/S0267-7261(02)00109-1.

[12] S. Molnar and J. F. Cassidy, "A comparison of site response techniques using weak-motion earthquakes and microtremors", Earthquake Spectra, 22(1), 169–188, (2006). DOI: 10.1193/1.2160502.

[13] E. Haghshenas, P.-Y. Bard and N. Theodulidis, "Empirical evaluation of microtremor H/V spectral ratio", Bulletin of Earthquake Engineering, 6(1), 75–108, (2008). DOI: 10.1007/s10518-007-9058-x.

[14] N. R. Draper and H. Smith, Applied Regression Analysis, 3rd ed. (Wiley, New York, 1998).

[15] D. C. Montgomery, E. A. Peck, and G. G. Vining, Introduction to Linear Regression Analysis, 5th ed. (Wiley, New York, 2012).

[16] M. H. Kutner, C. J. Nachtsheim, J. Neter, and W. Li, Applied Linear Statistical Models, 5th ed. (McGraw-Hill, New York, 2005).

[17] S. Weisberg, Applied Linear Regression, 3rd ed. (Wiley, New Jersey, 2005). DOI: 10.1002/0471704091

[18] G. Casella and R. L. Berger, Statistical Inference, 2nd ed. (Duxbury, Pacific Grove, 2002).

[19] A. Susilo, I. R. Ardiansyah, M. Z. Husni, "Site response and amplification factor analysis for earthquake hazard mitigation: A case study from Lombok Island", Journal of Physics: Conference Series, 2564, 012012, (2023). DOI: 10.1088/1742-6596/2564/1/012012.

[20] S. K. Ningrum, Z. Zulfakriza, S. Rosalia, S. Widiyantoro, "Amplification factors and resonance frequency mapping for seismic risk assessment in Indonesian urban areas", Geological Journal, 59(3), 842–856, (2024). DOI: 10.1002/gj.4891.

[21] A. Basso, M. Massa, G. Ferretti, "Statistical behavior of HVSR curves from large-scale seismic datasets: Log-normal distribution and power-law scaling", Bulletin of the Seismological Society of America, 105(2A), 920–932, (2015). DOI: 10.1785/0120140221.

[22] S. M. Mousavi, C. A. Langston, "Automatic noise-removal and signal-enhancement of seismic data using microtremor characteristics", Computers & Geosciences, 104, 10–21, (2017). DOI: 10.1016/j.cageo.2017.03.018.

[23] M. S. Admane, P. Murnal, "Logarithmic evaluation and outlier removal in site response analysis: Enhancing the reliability of H/V spectral ratios", Journal of Applied Geophysics, 201, 104635, (2022). DOI: 10.1016/j.jappgeo.2022.104635.

[24] E. H. Field and K. H. Jacob, "The theoretical response of sedimentary layers to ambient seismic noise", Geophysical Journal International, 113(3), 363–372, (1993). DOI: 10.1111/j.1365-246X.1993.tb00898.x.

[25] S. Parolai, U. Wegler and C. Milkereit, "Assessment of the stability of H/V spectral ratios from ambient vibrations and comparison with earthquake data in the Cologne area (Germany)", Tectonophysics, 390(1–4), 97–114, (2004). DOI: 10.1016/j.tecto.2004.03.031.

[26] F. Panzera, P. Bergamo and D. Fäh, "Canonical correlation analysis based on site-response proxies to predict site-specific amplification functions in Switzerland", Bulletin of the Seismological Society of America, 111, 1905–1920, (2021). DOI: 10.1016/j.tecto.2004.03.031.

[27] S. Bonnefoy-Claudet, F. Cotton and P.-Y. Bard, "The nature of noise wavefield and its applications for site effects studies: a literature review", Earth-Science Reviews, 79(3–4), 205–227, (2006).
DOI: 10.1016/j.earscirev.2006.07.004.

[28] T. Satoh, H. Kawase and S. Matsushima, "Estimation of S-wave velocity structures in and around the Sendai basin, Japan, using array records of microtremors", Bulletin of the Seismological Society of America, 91, 206–218, (2001). DOI: 10.1785/0120000002.

[29] M. A. Sarmadi, B. Hassani and S. López, "Evaluation of earthquake and microtremor HVSR methods for local site response estimation", Acta Geophysica, 69(2), 635–653, (2021). DOI: 10.1007/s11600-021-00561-1.

[30] B. Mi, Y. Wang and J. Hu, "Multistation HVSR and Rayleigh-wave analysis for shallow structure and site effect estimation", Soil Dynamics and Earthquake Engineering, 120, 361–375, (2019). DOI: 10.1016/j.soildyn.2019.01.036.

[31] M. Muzli, R. A. P. Kambali, J. Nugraha, S. Sulastri, A. R. Hakim, S. Rohadi, R. Triyono, N. F. Riama and D. Karnawati, "Site characterizations of BMKG seismic network, Indonesia, based on HVSR analysis", IOP Conference Series: Earth and Environmental Science, 873, 012025, (2021).

[32] G. Cultrera and A. Mercuri, "Statistical analysis of site effect indicators from the CRISP database: H/V spectral ratio of earthquake and noise data", Soil Dynamics and Earthquake Engineering, 185, 108129, (2025).

[33] C. M. Vidal, J. C. Komorowski, N. Metrich, I. Pratomo, N. Kartadinata, O. Prambada, M. Agnès, G. Carazzo, F. Lavigne, J. Rodysill, K. Fontijn and Surono, "Dynamics of the major plinian eruption of Samalas in 1257 A.D. (Lombok, Indonesia)", Bulletin of Volcanology, 77, (2015).

[34] M. Rong, H. Li and Y. Yu, "The difference between horizontal-to-vertical spectra ratio and empirical transfer function as revealed by vertical arrays", PLoS One, 14(1), e0210852, (2019).

[35] M. Subedi, R. M. Pokhrel, B. Pandey, D. P. N. Kontoni, "Nonlinear site response analysis and the impact of soil dynamic properties on seismic amplification during large earthquakes", Geosciences, 11(11), 452, (2021). DOI: 10.3390/geosciences11110452.

[36] D. Roten, D. Fäh, C. Cornou and D. Giardini, "Two-dimensional resonances in Alpine valleys identified from ambient vibration wavefields", Geophysical Journal International, 165(3), 889–905, (2006). DOI: 10.1111/j.1365-246X.2006.02935.x.

[37] C. Lachet and P.-Y. Bard, "Numerical and theoretical investigations on the possibilities and limitations of Nakamura's technique",

Journal of Physics of the Earth, 42(5), 377–397,
(1994). DOI: 10.15111/jpe.42.377.

Appendix

Table 1. MHVSR (microtremor) and EHVSR (earthquake) derived f_0 and A_0 values for seven BMKG stations on Lombok Island

No	Station	Parameter	Microtremor (HVSR)	Earthquake Recordings (EHVSR)
1	BYLI	f_0 (Hz)	0.858	0.894, 0.675, 1.005, 1.007, 0.937, 0.922, 0.937, 1.030, 0.934, 0.924, 0.696, 0.819, 0.857, 0.972, 1.134, 1.694, 0.930, 1.273, 0.734, 1.080, 0.791, 0.753, 0.802, 0.585, 0.896, 0.993, 1.041, 0.934, 0.924, 0.696, 0.857, 0.502, 0.780, 0.808, 0.539, 1.097, 0.782, 1.739, 1.642, 0.814, 0.836, 0.793, 0.784, 1.787, 0.860, 0.796, 0.906, 0.857, 0.807
		A_0	2.213	2.261, 2.313, 2.634, 2.323, 2.142, 2.156, 2.142, 2.400, 2.423, 2.121, 2.293, 2.483, 3.114, 2.492, 2.110, 2.569, 2.708, 2.035, 1.964, 2.200, 2.891, 3.257, 2.656, 2.539, 2.364, 2.463, 2.423, 2.121, 2.296, 3.114, 2.298, 2.700, 2.216, 2.617, 1.344, 2.282, 2.079, 2.230, 2.329, 2.754, 2.117, 2.431, 2.563, 2.061, 2.389, 2.394, 2.234, 2.372
2	KMNI	f_0 (Hz)	0.836	0.909, 0.765, 0.822, 0.779, 0.806, 0.851, 0.808, 0.646, 0.802, 0.798, 0.820, 0.833, 0.857, 0.851, 0.745, 0.865, 0.773, 0.833, 0.891, 0.898, 0.805, 0.898, 0.700, 0.843, 0.777, 0.784, 0.762, 0.842, 0.780, 0.797, 0.945, 0.803, 0.788, 0.795, 0.864, 0.867, 0.799, 0.823, 0.778, 0.810, 0.683
		A_0	6.98	5.970, 6.837, 8.526, 7.719, 7.499, 6.958, 7.519, 5.857, 6.309, 7.701, 7.767, 7.572, 7.359, 7.912, 7.014, 6.666, 8.229, 8.414, 6.651, 5.763, 7.978, 5.763, 6.950, 6.485, 6.613, 6.958, 7.060, 6.141, 6.674, 7.864, 4.386, 7.063, 7.341, 6.137, 4.388, 5.712, 2.383, 6.892, 6.489, 7.718, 5.692
3	PBLI	f_0 (Hz)	10.48	10.421, 10.323, 10.467, 10.525, 10.675, 9.999, 10.554, 9.750, 9.834, 9.798, 10.190, 10.120, 10.082, 9.835, 10.374, 10.058, 9.658, 9.219, 10.245, 9.943, 10.029, 10.220, 10.170, 10.049, 10.387
		A_0	5.19	5.618, 6.744, 6.010, 4.897, 4.482, 5.072, 5.922, 4.938, 5.089, 4.055, 3.990, 4.230, 3.587, 4.103, 6.531, 7.986, 3.529, 5.696, 4.723, 6.020, 4.729, 3.821, 4.960, 6.091
4	KLNI	f_0 (Hz)	14.44	14.469, 14.507, 14.510, 13.638, 14.473, 14.066, 14.507, 14.510, 14.176, 13.753, 14.365, 13.865, 13.987, 13.934, 13.903, 14.223, 14.507, 14.321, 14.435, 14.389, 14.214, 13.966, 13.820, 14.508, 14.041, 14.123, 14.322, 14.160, 13.905, 14.116, 14.381, 14.276, 14.129, 13.905
		A_0	3.48	3.595, 4.562, 3.442, 2.997, 3.469, 2.844, 3.884, 3.890, 3.611, 3.892, 3.152, 3.707, 4.491, 3.045, 3.550, 3.576, 3.850, 3.143, 3.444, 3.303, 3.166, 3.146, 3.612, 4.186, 4.340, 4.600, 4.498, 3.236, 3.114, 3.552, 3.408, 2.999, 3.506
5	LTNI	f_0 (Hz)	0.175	0.135, 0.159, 0.165, 0.213, 0.161, 0.168, 0.178, 0.168, 0.165, 0.156, 0.160, 0.159, 0.190, 0.165, 0.247, 0.207, 0.190, 0.187, 0.158, 0.279, 0.182, 0.191, 0.168, 0.204, 0.256, 0.206, 0.187, 0.136, 0.220, 0.162, 0.182, 0.170, 0.185, 0.195, 0.181, 0.184, 0.182, 0.184
		A_0	1.84	3.430, 2.448, 2.660, 2.480, 3.168, 2.121, 2.687, 2.987, 2.625, 2.728, 2.860, 2.930, 2.150, 1.667, 1.314, 2.240, 2.150, 2.556, 2.749, 1.979, 1.771, 2.093, 2.214, 2.432, 2.424, 3.033, 2.092, 1.895, 2.029, 2.453, 2.048, 2.064, 2.516, 2.373, 1.831, 2.950, 2.475
6	SLBFM	f_0 (Hz)	1.82	1.783, 1.832, 1.896, 1.623, 1.878, 1.995, 1.836, 1.804, 1.771, 1.787, 1.831, 1.778, 1.890, 1.924, 1.904, 1.766, 1.793, 1.843, 1.757, 1.847, 1.908, 1.864, 1.833, 1.860, 1.926, 1.857, 1.776, 1.872, 1.796, 1.859, 1.764, 1.791, 1.910, 1.871, 1.886, 1.932, 1.935, 1.861, 1.805, 1.919

		A_0	6.7	6.619, 6.017, 6.444, 8.112, 6.492, 6.030, 6.352, 7.883, 5.567, 7.109, 6.278, 5.461, 5.045, 7.689, 6.314, 6.177, 6.556, 7.339, 4.921, 7.290, 6.081, 6.047, 7.179, 6.881, 6.359, 5.625, 6.978, 6.489, 6.189, 5.903, 6.159, 6.765, 6.217, 7.585, 4.717, 6.909, 6.815, 6.221, 7.330, 6.489
7	WLTFM	f_0 (Hz)	4.558	4.699, 4.418, 4.310, 4.318, 4.467, 3.998, 4.204, 4.384, 4.564, 4.117, 4.258, 4.335, 4.250, 4.412, 4.596, 4.317, 4.495, 4.306, 4.124, 3.935, 4.348, 4.381, 4.527, 4.385, 4.056, 4.588, 4.372, 5.080, 4.349, 4.372, 4.407, 4.430, 4.340, 4.408, 4.491, 4.439, 4.389, 4.401, 4.524, 4.287, 4.832, 4.455, 4.390, 4.633, 4.320
		A_0	3.826	4.481, 3.617, 4.293, 3.881, 3.780, 4.014, 3.710, 3.865, 3.725, 4.318, 3.805, 3.938, 4.212, 3.844, 3.702, 3.908, 4.042, 4.124, 3.838, 3.719, 4.310, 3.518, 4.154, 4.182, 3.778, 4.011, 3.826, 4.096, 4.312, 3.264, 3.736, 3.385, 3.336, 3.665, 4.170, 2.971, 3.778, 3.893, 3.703, 3.063, 3.879, 4.326, 3.676, 3.896, 4.812, 4.312